Heart and Vessels (2023) 38:90–95
https://doi.org/10.1007/s00380-022-02125-9

ORIGINAL ARTICLE

Ablation index-guided high-power vs. moderate-power cavotricuspid isthmus ablation

Akio Chikata[1,2] · Takeshi Kato[2] · Kazuo Usuda[1] · Shuhei Fujita[3] · Michiro Maruyama[1] · Kanichi Otowa[1] · Keisuke Usuda[2] · Takashi Kusayama[2] · Toyonobu Tsuda[2] · Kenshi Hayashi[2] · Masayuki Takamura[2]

Received: 3 April 2022 / Accepted: 15 June 2022 / Published online: 19 July 2022

Abstract

Ablation index (AI)-guided ablation is useful for pulmonary vein isolation (PVI) and cavotricuspid isthmus (CTI) ablation. However, the impact of radiofrequency (RF) application power on CTI ablation with a fixed target AI remains unclear. One-hundred-thirty drug-refractory atrial fibrillation and/or atrial flutter patients who underwent AI-guided CTI ablation with or without PVI between July 2020 and August 2021 were randomly assigned to high-power (45 W) and moderate-power (35 W) groups. We performed CTI ablation with the same target AI value in both groups: 500 for the anterior 1/3 segments and 450 for the posterior 2/3 segments. In total, first-pass conduction block of the CTI was obtained in 111 patients (85.4%), with 7 patients (5.4%) showing CTI reconnection. The rate of first-pass conduction block was significantly higher in the 45 W group (61/65, 93.8%) than in the 35 W group (50/65, 76.9%, P = 0.01). CTI ablation and CTI fluoroscopy time were significantly shorter in the 45 W group than in the 35 W group (CTI ablation time: 192.3 ± 84.8 vs. 319.8 ± 171.4 s, P < 0.0001; CTI fluoroscopy time: 125.2 ± 122.4 vs. 171.2 ± 124.0 s, P = 0.039). Although there was no significant difference, steam pops were identified in two patients from the 45 W group at the anterior segment of the CTI. The 45 W ablation strategy was faster and provided a higher probability of first-pass conduction block than the 35 W ablation strategy for CTI ablation with a fixed AI target.

Keywords Ablation index · High-power short-duration · Cavotricuspid isthmus

Introduction

Radiofrequency (RF) ablation of the cavotricuspid isthmus (CTI) is an established treatment for CTI-dependent right atrial flutter (AFL). Although the success rate for CTI ablation is high, it can be difficult to achieve bidirectional conduction block in some patients [1]. Transmural lesions without excessive collateral damage are necessary to achieve effective ablation without complications. The lesion size is affected by catheter stability, contact force (CF), power, and duration of energy application [2]. The ablation index (AI) (CARTO 3 V4, Biosense Webster, Inc., Diamond Bar, CA, USA) is a novel marker of lesion quality that incorporates CF, time, and power in a weighted formula and is shown to accurately estimate lesion depth [3]. AI-guided ablation is associated with significant improvements in first-pass isolation for pulmonary vein isolation (PVI), first-pass conduction block for CTI ablation, and atrial tachyarrhythmia recurrence [4–7]. Utility and low complication rates using high power for a short duration for atrial fibrillation (AF) ablations have been recently reported [8–11]. High-power application is also associated with a higher first-pass PVI for the same AI target [12]. A power of 35–50 W and a temperature limit of 40 °C–45 °C are generally used for CTI ablation with irrigated catheters [13–17]. However, the impact of RF application power on CTI ablation with a fixed target AI has not been fully investigated.

Here, we conducted a prospective randomized study comparing the efficacy and safety of two different RF powers for AI-guided CTI ablation.

✉ Takeshi Kato
takeshikato@me.com

[1] Department of Cardiology, Toyama Prefectural Central Hospital, Toyama, Japan

[2] Department of Cardiovascular Medicine, Kanazawa University Graduate School of Medical Sciences, 13-1 Takara-machi, Kanazawa 920-8641, Japan

[3] Department of Pediatrics, Toyama Prefectural Central Hospital, Toyama, Japan

Methods

Study subjects

This single-center randomized trial included patients managed between July 2020 and August 2021 in the Toyama Prefectural Central Hospital. Participants included patients aged ≥ 18 years who underwent either CTI ablation for the treatment of isthmus-dependent AFL or CTI ablation as a part of AF treatment. We excluded patients who had previously undergone CTI ablation and those with second- or third-degree atrioventricular block. We also excluded patients who could not undergo contrast-enhanced 3D CT imaging. The primary efficacy endpoint was the establishment of a first-pass conduction block. First-pass conduction block was defined as a bidirectional conduction block of the CTI that occurred either before or at the completion of the CTI line ablation without the need for additional ablation [6]. Secondary safety endpoints included periprocedural complications, CTI ablation time, and CTI fluoroscopy time.

Patients were randomly assigned to the ablation protocol given 45 or 35 W for the same target AI value. All patients gave written informed consent before enrollment in the study. The trial was approved by the local ethics committee and registered in the UMIN Clinical Trials Registry (000,045,351).

Anatomical analysis of CTI using CT image

The anatomical features of the CTI were evaluated using contrast-enhanced 3D CT images. Reconstruction CT images of right anterior oblique (RAO) 30° and left anterior oblique (LAO) 60° projections were used to evaluate CTI morphology. The morphology of CTI was divided into three categories according to previous studies [18, 19]. A flat CTI was defined as a straight area with an inferior concavity measuring 2 mm or less between the IVC and TV. A concave CTI was defined as an inferior concavity more than 2 mm without the vestibular area. A pouched CTI was defined when the CTI had a vestibular area and a distinct inferior pouch. The CTI length, length of the vestibular area, depth of the pouch, and concavity were measured in the RAO 30° view (Fig. 1).

CTI ablation procedure

All procedures were performed under conscious sedation. A 20-electrode atrial cardioversion catheter was inserted using the left cubital approach and positioned in the coronary sinus [20]. In patients with AF, transseptal puncture was performed under the guidance of intracardiac ultrasound.

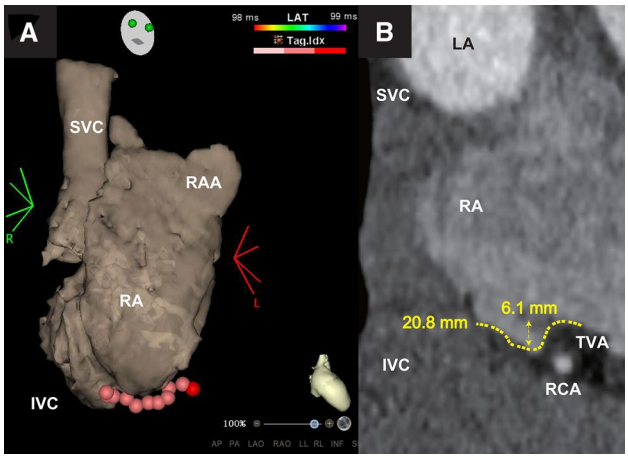

Fig. 1 Right anterior oblique (RAO) view of three-dimensional merged computed tomography using the CARTO 3 system (**A**) and a slice of CT images in the RAO direction of cavotricuspid isthmus (CTI) (**B**). CT images showed that CTI has a 6.1-mm depth pouch. Red dots represent ablation lesions with AI values ≥ 500. *LA* left atrium, *SVC* superior vena cava, *RA* right atrium, *TVA* tricuspid valve annulus, *RCA* right coronary artery, *IVC* inferior vena cava.

An 8-Fr long sheath (SL0; St. Jude Medical, St. Paul, MN, USA) and steerable sheaths (Agilis; St. Jude Medical, Inc.) or VIZIGO sheaths (Biosense Webster, Inc., Irvine, CA, USA) were placed into the left atrium. A SmartTouch SF catheter (Biosense Webster, Inc., Irvine, CA, USA) was introduced. Then, extensive encircling of the ipsilateral PVI was performed, guided by 3D-US geometries and 3DMerge CT using the CARTO 3 system (Biosense Webster, Inc.). In patients with AFL during the procedure, entrainment maneuvers were performed to confirm CTI dependence, whereas in patients with sinus rhythm, empiric CTI ablation was performed during pacing from the proximal coronary sinus at 600 ms. Agilis sheaths or VIZIGO sheaths and SmartTouch SF were also used for CTI ablation. The CTI ablation line was along the 5:30 to 6:30 AM region of the fluoroscopic left anterior oblique view, targeted to ablate the inferior isthmus. Ablation index-guided point-by-point linear ablation was performed starting from the tricuspid valve annulus to the inferior cava veins.

The VisiTag settings were as follows: minimum time, 3 s; maximum distance change, 2.5 mm; minimum force, 3 g; and force over time, 30%. The mean CF (g), power (W), impedance drop (Ω), ablation time (s), force–time integral (FTI; gs), and AI of every VisiTag point were automatically recorded during ablation. The maximal inter-lesion distance (ILD) between two neighboring lesions was less than 4 mm. The power settings were 45 W or 35 W with saline irrigation at a flow rate of 15 mL/min and a temperature limit of 40 °C. In case of a sudden increase in CF or impedance rise, we stopped RF application. We performed CTI ablation with the same target AI value in both groups: 500 for anterior

1/3 segments and 450 for posterior 2/3 segments, with a CF of 10 to 30 g (Fig. 1). First-pass conduction block was defined as a bidirectional conduction block of the CTI that occurred either before or at the completion of CTI line ablation without the need for additional ablatio [6]. The endpoint of ablation was a transisthmus conduction block with widely spaced double potentials and bidirectional block by pacing from the proximal coronary sinus and inferior lateral right atrium, which was continuously reevaluated for 15 min or more after CTI ablation.

Statistical analysis

Statistical analyses were performed using GraphPad Prism (GraphPad Software, La Jolla, CA, USA) and SPSS 22.0 (IBM Corp., Armonk, NY, USA). Data are reported as mean ± standard deviation. Data were compared using Student's *t* tests to examine the differences between the two groups. All analyses were two-sided. A *P* value of < 0.05 was considered statistically significant. We considered an absolute 20% difference in the rate of the first-pass conduction block. We assumed a first-pass conduction block rate of 90% in the 45 W group and 70% in the 35 W group. To achieve a statistical power of 80% with a level set to 0.05, 62 patients for each group were needed for superiority, and we planned to include 65 patients for each group.

Results

Study population

A total of 130 patients with symptomatic, drug-refractory AF and/or AFL were enrolled. Sixty-five patients each were randomly assigned to the two study groups. The baseline characteristics of the patients are shown in Table 1. There were no significant differences between the two groups regarding clinical characteristics or cardiac function evaluated by echocardiography.

Outcomes

The procedural characteristics are summarized in Table 2. In total, first-pass conduction block of the CTI was obtained in 111 patients (85.4%), with 7 patients (5.4%) showing CTI reconnection during the waiting period after the ablation. The CTI block at the end of the procedure was achieved in all patients. The rate of first-pass conduction block of the CTI was significantly higher in the 45 W group (61/65, 93.8%) than in the 35 W group (50/65, 76.9%, $P = 0.01$). During the waiting period, spontaneous CTI reconnection was observed in three (4.6%) patients from the 45 W group and four (6.2%) patients from the 35 W group ($P = 1.00$).

Table 1 Patient characteristics

Patient characteristic	45 W group ($n = 65$)	35 W group ($n = 65$)	*p* value
Age, years	68.5 ± 10.6	69.0 ± 10.0	0.76
Male, *n* (%)	42 (64.6)	42 (64.6)	1.00
Height, cm	162.1 ± 9.4	162.8 ± 10.2	0.69
Body weight, kg	63.1 ± 12.3	63.7 ± 10.9	0.77
Body mass index, kg/m^2	23.9 ± 3.7	24.0 ± 3.2	0.92
Hypertension, *n* (%)	40 (61.5)	34 (52.3)	0.38
Diabetes mellitus, *n* (%)	10 (15.4)	6 (9.2)	0.42
Ischemic heart disease, *n* (%)	3 (4.6)	7 (10.8)	0.32
Congestive heart failure, *n* (%)	28 (43.1)	26 (40)	0.86
CHA_2DS_2-VASc-score, *n* (%)			
0	4 (6.2)	7 (10.8)	0.53
1	11 (16.9)	6 (9.2)	0.30
≥ 2	50 (76.9)	52 (80)	0.83
Left ventricular ejection fraction, %	62.4 ± 12.4	62.7 ± 11.5	0.87
Left atrial diameter, mm	40.0 ± 6.8	40.5 ± 7.7	0.69
BNP, pg/ml	130.8 ± 155.5	112.3 ± 108.7	0.44
eGFR Cockcroft-Gault, ml/min	58.9 ± 18.9	56.3 ± 16.6	0.41
DOAC, *n* (%)	63 (96.9)	62 (95.4)	1.00

BNP B-type natriuretic peptide, *eGFR* estimated glomerular filtration rate, *DOAC* direct oral anticoagulant, *Na* sodium

There were no major procedural complications, except for one pseudoaneurysm in the 35 W group. The CTI ablation and CTI fluoroscopy time were significantly shorter in the 45 W group than in the 35 W group (CTI ablation time: 192.3 ± 84.8 vs. 319.8 ± 171.4 s, $P < 0.0001$; CTI fluoroscopy time: 125.2 ± 122.4 vs. 171.2 ± 124.0 s, $P = 0.039$).

Anatomical features of Cavotricuspid isthmus assessed by computed tomography

CTI length measured using CT was not different between the two groups (30.3 ± 9.1 vs. 28.3 ± 8.2 mm, $P = 0.2$, Table 3). Furthermore, CTI morphology was not different between the two groups (Table 3).

Evaluation of VisiTag parameters

Table 4 shows VisiTag data for the two groups. In total, 935 points in the 45 W group and 945 points in 35 W were analyzed. There was no difference in AI between the 45 W group and the 35 W group both in total and each segment. RF application time was shorter and FTI was smaller in the 45 W group than in the 35 W group in the total and segmental analysis. ILD and CF were not different between the two groups in the overall analysis. However, ILD was

Table 2 Primary and secondary endpoints

	45 W group ($n=65$)	35 W group ($n=65$)	p value
PVI, n (%)	59 (90.8)	57 (87.7)	0.78
Other than PVI except CTI, n (%)	18 (27.7)	14 (21.5)	0.54
CTI block at the end of procedure, n (%)	100 (100)	100 (100)	1.00
Primary efficacy endpoint			
First-pass conduction block, n (%)	61 (93.8)	50 (76.9)	0.01
Acute reconnection, n (%)	3 (4.6)	4 (6.2)	1.00
Secondary safety endpoint			
CTI fluoroscopy time, s	125.2 ± 122.4	171.2 ± 124.0	0.04
CTI Ablation time, s	192.3 ± 84.8	319.8 ± 171.4	< 0.0001
Access site complication, n (%)	0 (0)	1 (1.5)	1.00
Cardiac tamponade, n (%)	0 (0)	0 (0)	1.00
Symptomatic cerebral infarction, n (%)	0 (0)	0 (0)	1.00

Table 3 Anatomical features of cavotricuspid isthmus

	45 W group ($n=65$)	35 W group ($n=65$)	p value
CTI length, mm	30.3 ± 9.1	28.3 ± 8.2	0.20
CTI morphology			
Pouch, n (%)	21 (32.3)	18 (27.7)	0.70
Flat, n (%)	17 (26.2)	17 (26.2)	1.00
Concave, n (%)	22 (33.8)	25 (38.5)	0.72
Length of vestibular area, mm	10.2 ± 2.8	9.3 ± 3.4	0.39
Depth of sub-Eustachian pouch, mm	5.1 ± 1.4	5.1 ± 2.3	0.99
Depth of concave, mm	5.7 ± 1.6	5.6 ± 1.6	0.79

significantly longer in the 45 W group at the anterior segment, and CF was significantly lower in the 45 W group at the middle and posterior segments. Although there was no significant difference, steam pops were perceived in two patients from the 45 W group at the anterior segment of flat CTI. The ablation parameter at steam pop sites were: (a) power 45 W, duration 13 s, impedance drop 17 Ω, CF 22 g, AI = 504, in 71-year-old female patient, and (b) power 45 W, duration 15 s, impedance drop 13 Ω, CF 16 g, AI = 493, in 68-year-old male patient. During the in-hospital and the following 3-month observation, no major adverse events including cardiac tamponade were found in these patients.

Discussion

This study evaluated the impact of RF application power settings on the acute results of AI-guided CTI ablation for the same target value. Our major findings were as follows: (1) First-pass conduction block of CTI was significantly higher in the 45 W group than in the 35 W group despite the same target ABI value; (2) the 45 W group required less RF and fluoroscopy time than the 35 W group; and (3) although no major cardiac complications occurred, steam pops were observed in two patients from the 45 W group.

In this study, first-pass conduction block was more frequently achieved in the 45 W group than in the 35 W group for the same target ABI value. The AI target values were 500 for the anterior 1/3 segment and 450 for the posterior 2/3 segment, while ILD was 4 mm. The utility of AI-guided CTI ablation has been previously reported [6, 7]. In those studies, the AI targets were set at 500 for the anterior 2/3 segment and 400–500 for the posterior 1/3 segment, while ILD was 6 mm. In this study, the target AI value in the middle section was slightly lower than in previous studies. Since the thinnest area of myocardial wall thickness in CTI is reported to be the central isthmus [21], we set the target AI for the middle section lower than previous reports to avoid collateral damage.

RF power settings were set between 35 and 40 W in previous AI-guided CTI ablation studies [6, 7], and between 35 and 50 W in studies without AI guidance [13–17]. First-pass conduction block was reached in 88.3–93.0% of AI-guided CTI ablation studies [6.7]. In this study, first-pass conduction block was obtained in 111 patients (85.4%) when the RF power was set to 35 or 45 W, which is comparable to previous reports. The effectiveness and safety of high-power short-duration (HPSD) ablation for CTIs have also been reported [22]. Kwon et al. compared a 50 W for 15 s strategy and 30 W for 60 s strategy and reported that the first-pass conduction block rate was similar, but the RF application time was shorter in 50 W for 15 s. They compared different RF settings but did not evaluate CF and AI. In the present study, we evaluated the effect of different RF power settings with the same target AI value; first-pass conduction block of the CTI was significantly higher in the 45 W group.

Table 4 Characteristics of each ablation point

	45 W group ($n=65$)	35 W group ($n=65$)	p value
Number of application for CTI block, n	14.8 ± 6.1	17.2 ± 8.6	0.07
Number of VisiTag points			
Total, n	935	945	
Anterior, n	276	287	
Middle, n	337	360	
Posterior, n	322	298	
RF application time per VisiTag points, s			
Total	13.0 ± 4.8	18.8 ± 6.7	< 0.0001
Anterior	15.5 ± 5.6	21.8 ± 7.3	< 0.0001
Middle	13.0 ± 4.1	18.3 ± 5.4	< 0.0001
Posterior	10.9 ± 4.0	16.6 ± 6.4	< 0.0001
Contact force, g			
Total	16.7 ± 6.1	17.1 ± 6.4	0.19
Anterior	15.3 ± 4.5	16.4 ± 5.0	0.005
Middle	16.1 ± 5.6	17.0 ± 6.1	0.038
Posterior	18.6 ± 7.3	17.8 ± 7.8	0.22
FTI, gs			
Total	200.1 ± 57.7	296.6 ± 89.0	< 0.0001
Anterior	229.9 ± 69.7	339.7 ± 100.8	< 0.0001
Middle	192.7 ± 46.1	285.4 ± 82.3	< 0.0001
Posterior	184.6 ± 52.4	263.1 ± 76.9	< 0.0001
AI			
Total	449.0 ± 51.6	446.4 ± 51.0	0.27
Anterior	471.0 ± 61.6	467.4 ± 60.9	0.49
Middle	447.1 ± 37.2	445.3 ± 36.8	0.51
Posterior	432.1 ± 48.4	427.6 ± 47.8	0.24
ILD, mm			
Total	3.93 ± 1.54	3.84 ± 1.54	0.22
Anterior	4.02 ± 1.51	3.73 ± 1.35	0.02
Middle	3.88 ± 1.52	3.85 ± 1.65	0.84
Posterior	3.93 ± 1.56	3.93 ± 1.56	0.96
GAP, n (%)			
Total	4 (0.4)	17 (1.8)	0.007
Anterior	0 (0)	5 (1.7)	0.06
Middle	4 (1.2)	10 (2.8)	0.18
Posterior	0 (0)	2 (0.7)	0.23
Acute reconnection, n (%)			
Total	3 (0.3)	4 (0.4)	1.00
Anterior	1 (0.4)	1 (0.3)	1.00
Middle	0 (0)	2 (0.6)	0.50
Posterior	2 (0.6)	1 (0.3)	1.00
Pop, n (%)			
Total	2 (0.2)	0 (0)	0.24
Anterior	2 (0.7)	0 (0)	0.51
Middle	0 (0)	0 (0)	1.00
Posterior	0 (0)	0 (0)	1.00

HPSD ablation causes immediate irreversible tissue damage and reduces the conductive phase to minimize collateral damage. HPSD ablation creates lesions that are similar in volume but broader and less deep than the standard power and duration [23–25]. Catheter stability during RF application is also a crucial determinant of lesion formation. Longer duration energy applications may be associated with compromised stability of catheter contact [26]. In this study, the RF application time for each point was shorter in the 45 W group than in the 35 W group to achieve the same AI value. This might lead to a higher rate of first-pass conduction block in the 45 W group, despite the lower CF and longer ILD in some segments.

High-power RF applications may increase the risk of steam pop. In 2 of the 65 patients from the 45 W group, steam pops were noted; all occurred while ablating the anterior CTI segment with approximately 500 AI value. Although no pericardial effusion or cardiac tamponade was observed, high-power RF application with an AI value above 500 may increase the risk for steam pop.

Study limitations

The present study has several limitations. First, this was a single-center study with a relatively small sample size. Thus, larger multicenter studies are needed to confirm our findings. Second, we only evaluated the acute efficacy and safety of the procedure; the long-term results remain unknown.

Conclusions

In CTI ablation using a fixed ABI target, the 45 W ablation strategy was faster and provided a higher probability of first-pass conduction block than the 35 W ablation strategy under the same AI target value.

Funding None.

Declarations

Conflict of interest The authors declare that they have no conflict of interest.

References

1. Asirvatham SJ (2009) Correlative anatomy and electrophysiology for the interventional electrophysiologist: right atrial flutter. J Cardiovasc Electrophysiol 20:113–122
2. Ikeda A, Nakagawa H, Lambert H, Shah DC, Fonck E, Yulzari A, Sharma T, Pitha JV, Lazzara R, Jackman WM (2014) Relationship between catheter contact force and radiofrequency lesion size and incidence of steam pop in the beating canine heart: electrogram

amplitude, impedance, and electrode temperature are poor predictors of electrode-tissue contact force and lesion size. Circ Arrhythm Electrophysiol 7:1174–1180
3. Das M, Loveday JJ, Wynn GJ, Gomes S, Saeed Y, Bonnett LJ, Waktare JEP, Todd DM, Hall MCS, Snowdon RL, Modi S, Gupta D (2017) Ablation index, a novel marker of ablation lesion quality: prediction of pulmonary vein reconnection at repeat electrophysiology study and regional differences in target values. Europace 19:775–783
4. Hussein A, Das M, Chaturvedi V, Asfour IK, Daryanani N, Morgan M, Ronayne C, Shaw M, Snowdon R, Gupta D (2017) Prospective use of Ablation Index targets improves clinical outcomes following ablation for atrial fibrillation. J Cardiovasc Electrophysiol 28:1037–1047
5. Taghji P, El Haddad M, Phlips T, Wolf M, Knecht S, Vandekerckhove Y, Tavernier R, Nakagawa H, Duytschaever M (2018) Evaluation of a strategy aiming to enclose the pulmonary veins with contiguous and optimized radiofrequency lesions in paroxysmal atrial fibrillation: a pilot study. JACC Clin Electrophysiol 4:99–108
6. Zhang T, Wang Y, Han Z, Zhao H, Liang Z, Wang Y, Wu Y, Ren X (2019) Cavotricuspid isthmus ablation using ablation index in typical right atrial flutter. J Cardiovasc Electrophysiol 30:2414–2419
7. Viola G, Stabile G, Bandino S, Rossi L, Marrazzo N, Pecora D, Bottoni N, Solimene F, Schillaci V, Scaglione M, Ocello S, Baiocchi C, Santoro A, Donzelli S, De Ruvo E, Lavalle C, Sanchez-Gomez JM, Pastor JFA, Grandio PC, Ferraris F, Castro A, Rebellato L, Marchese P, Adao L, Primo J, Barra S, Casu G (2021) Safety, efficacy, and reproducibility of cavotricuspid isthmus ablation guided by the ablation index: acute results of the FLAI study. Europace 23:264–270
8. Winkle RA, Mohanty S, Patrawala RA, Mead RH, Kong MH, Engel G, Salcedo J, Trivedi CG, Gianni C, Jais P, Natale A, Day JD (2019) Low complication rates using high power (45–50 W) for short duration for atrial fibrillation ablations. Heart Rhythm 16:165–169
9. Berte B, Hilfiker G, Russi I, Moccetti F, Cuculi F, Toggweiler S, Ruschitzka F, Kobza R (2019) Pulmonary vein isolation using a higher power shorter duration CLOSE protocol with a surround flow ablation catheter. J Cardiovasc Electrophysiol 30:2199–2204
10. Winkle RA (2021) HPSD ablation for AF high-power short-duration RF ablation for atrial fibrillation: a review. J Cardiovasc Electrophysiol 32:2813–2823
11. Ravi V, Poudyal A, Abid QU, Larsen T, Krishnan K, Sharma PS, Trohman RG, Huang HD (2021) High-power short duration vs. conventional radiofrequency ablation of atrial fibrillation: a systematic review and meta-analysis. Europace 23:710–721
12. Okamatsu H, Koyama J, Sakai Y, Negishi K, Hayashi K, Tsurugi T, Tanaka Y, Nakao K, Sakamoto T, Okumura K (2019) High-power application is associated with shorter procedure time and higher rate of first-pass pulmonary vein isolation in ablation index-guided atrial fibrillation ablation. J Cardiovasc Electrophysiol 30:2751–2758
13. Jaïs P, Haïssaguerre M, Shah DC, Takahashi A, Hocini M, Lavergne T, Lafitte S, Le Mouroux A, Fischer B, Clémenty J (1998) Successful irrigated-tip catheter ablation of atrial flutter resistant to conventional radiofrequency ablation. Circulation 98:835–838
14. Atiga WL, Worley SJ, Hummel J, Berger RD, Gohn DC, Mandalakas NJ, Kalbfleisch S, Halperin H, Donahue K, Tomaselli G, Calkins H, Daoud E (2002) Prospective randomized comparison of cooled radiofrequency versus standard radiofrequency energy for ablation of typical atrial flutter. Pacing Clin Electrophysiol 25:1172–1178
15. Scavée C, Jaïs P, Hsu LF, Sanders P, Hocini M, Weerasooriya R, Macle L, Raybaud F, Clementy J, Haïssaguerre M (2004) Prospective randomised comparison of irrigated-tip and large-tip catheter ablation of cavotricuspid isthmus-dependent atrial flutter. Eur Heart J 25:963–969
16. Ventura R, Klemm H, Lutomsky B, Demir C, Rostock T, Weiss C, Meinertz T, Willems S (2004) Pattern of isthmus conduction recovery using open cooled and solid large-tip catheters for radiofrequency ablation of typical atrial flutter. J Cardiovasc Electrophysiol 15:1126–1130
17. Ilg KJ, Kühne M, Crawford T, Chugh A, Jongnarangsin K, Good E, Pelosi F Jr, Bogun F, Morady F, Oral H (2011) Randomized comparison of cavotricuspid isthmus ablation for atrial flutter using an open irrigation-tip versus a large-tip radiofrequency ablation catheter. J Cardiovasc Electrophysiol 22:1007–1012
18. Saremi F, Pourzand L, Krishnan S, Ashikyan O, Gurudevan SV, Narula J, Kaushal K, Raney A (2008) Right atrial cavotricuspid isthmus: anatomic characterization with multi-detector row CT. Radiology 247:658–668
19. Kajihara K, Nakano Y, Hirai Y, Ogi H, Oda N, Suenari K, Makita Y, Sairaku A, Tokuyama T, Motoda C, Fujiwara M, Watanabe Y, Kiguchi M, Kihara Y (2013) Variable procedural strategies adapted to anatomical characteristics in catheter ablation of the cavotricuspid isthmus using a preoperative multidetector computed tomography analysis. J Cardiovasc Electrophysiol 24:1344–1351
20. Chikata A, Kato T, Usuda K, Fujita S, Maruyama M, Otowa KI, Takashima SI, Murai H, Usui S, Furusho H, Kaneko S, Takamura M (2019) Coronary sinus catheter placement via left cubital vein for phrenic nerve stimulation during pulmonary vein isolation. Heart Vessels 34:1710–1716
21. Baccillieri MS, Rizzo S, De Gaspari M, Paradiso B, Thiene G, Verlato R, Basso C (2019) Anatomy of the cavotricuspid isthmus for radiofrequency ablation in typical atrial flutter. Heart Rhythm 16:1611–1618
22. Kwon HJ, Lee SS, Park YJ, Park SJ, Park KM, Kim JS, On YK (2020) Effectiveness and safety of high-power and short-duration ablation for cavotricuspid isthmus ablation in atrial flutter. Pacing Clin Electrophysiol 43:941–946
23. Barkagan M, Contreras-Valdes FM, Leshem E, Buxton AE, Nakagawa H, Anter E (2018) High-power and short-duration ablation for pulmonary vein isolation: Safety, efficacy, and long-term durability. J Cardiovasc Electrophysiol 29:1287–1296
24. Bourier F, Duchateau J, Vlachos K, Lam A, Martin CA, Takigawa M, Kitamura T, Frontera A, Cheniti G, Pambrun T, Klotz N, Denis A, Derval N, Cochet H, Sacher F, Hocini M, Haïssaguerre M, Jais P (2018) High-power short-duration versus standard radiofrequency ablation: Insights on lesion metrics. J Cardiovasc Electrophysiol 29:1570–1575
25. Leshem E, Zilberman I, Tschabrunn CM, Barkagan M, Contreras-Valdes FM, Govari A, Anter E (2018) High-power and short-duration ablation for pulmonary vein isolation: biophysical characterization. JACC Clin Electrophysiol 4:467–479
26. Yavin HD, Leshem E, Shapira-Daniels A, Sroubek J, Barkagan M, Haffajee CI, Cooper JM, Anter E (2020) Impact of High-Power Short-Duration Radiofrequency Ablation on Long-Term Lesion Durability for Atrial Fibrillation Ablation. JACC Clin Electrophysiol 6:973–985